Baseline reward circuitry activity and trait reward responsiveness predict expression of opioid analgesia in healthy subjects

Vishvarani Wanigasekera[a,1], Michael C. Lee[a,b], Richard Rogers[a], Yazhuo Kong[a], Siri Leknes[a,c], Jesper Andersson[a], and Irene Tracey[a]

[a]Centre for Functional Magnetic Resonance Imaging of the Brain, Nuffield Department of Clinical Neurosciences, Nuffield Division of Anaesthetics, University of Oxford, John Radcliffe Hospital, Headington, Oxford OX3 9DU, United Kingdom; [b]Division of Anaesthesia, Department of Medicine, University of Cambridge, Cambridge CB2 1TN, United Kingdom; and [c]Department of Psychology, University of Oslo, 0317 Oslo, Norway

Edited by Howard L. Fields, University of California at San Francisco, Emeryville, CA, and accepted by the Editorial Board August 8, 2012 (received for review December 12, 2011)

Variability in opioid analgesia has been attributed to many factors. For example, genetic variability of the μ-opioid receptor (MOR)-encoding gene introduces variability in MOR function and endogenous opioid neurotransmission. Emerging evidence suggests that personality trait related to the experience of reward is linked to endogenous opioid neurotransmission. We hypothesized that opioid-induced behavioral analgesia would be predicted by the trait reward responsiveness (RWR) and the response of the brain reward circuitry to noxious stimuli at baseline before opioid administration. In healthy volunteers using functional magnetic resonance imaging and the μ-opioid agonist remifentanil, we found that the magnitude of behavioral opioid analgesia is positively correlated with the trait RWR and predicted by the neuronal response to painful noxious stimuli before infusion in key structures of the reward circuitry, such as the orbitofrontal cortex, nucleus accumbens, and the ventral tegmental area. These findings highlight the role of the brain reward circuitry in the expression of behavioral opioid analgesia. We also show a positive correlation between behavioral opioid analgesia and opioid-induced suppression of neuronal responses to noxious stimuli in key structures of the descending pain modulatory system (amygdala, periaqueductal gray, and rostral–ventromedial medulla), as well as the hippocampus. Further, these activity changes were predicted by the preinfusion period neuronal response to noxious stimuli within the ventral tegmentum. These results support the notion of future imaging-based subject-stratification paradigms that can guide therapeutic decisions.

functional MRI | functional imaging | endophenotype

Opioids are the mainstay of moderate to severe pain management, but there is considerable variation in the analgesic response leading to inadequate analgesia for many patients (1). This variability has been attributed to many factors including the genetic variability of the μ-opioid receptor (MOR)-encoding gene that introduces variability in MOR function and endogenous opioid neurotransmission (2). Endogenous opioid neurotransmission mediates exogenous opioid analgesia (3), increases in response to noxious stimuli reducing the unpleasantness of noxious stimuli (4), enhances the pleasantness of rewarding stimuli (5), and influences the responsiveness of an individual to rewards (6). Therefore, endogenous opioids play a central role not only in mediating exogenous opioid analgesia, but also in endogenous modulation of pain perception and reward processing.

Reward is not one simple construct, and there are many different types of reward such as monetary gain, palatable food, mood enhancing drugs, and social reward. An increasingly well-identified set of brain regions consisting of the anterior cingulate cortex (ACC), orbitofrontal cortex (OFC), the ventral striatum, ventral pallidum, and the midbrain tegmentum as well as the prefrontal cortex, amygdala and the hippocampus are differentially involved in processing these many types of rewards (7). Further, activation in these brain regions are differentially involved in processing different aspects of reward such as prediction of (8, 9), anticipation of (10), and magnitude of (11) reward. Analgesia is rewarding and indeed human imaging studies demonstrate the role of the accumbens in anticipation of analgesia where the reward was placebo analgesia (12) and in predicting analgesia where the reward was offset analgesia (13). Crucially, several of these structures, both in humans (14, 15) and in animals (16–18), also contain MORs and play a role in opioid-induced behavioral analgesia.

These combined observations strongly suggest that behavioral opioid analgesia depends on endogenous opioid neurotransmission and involves components of the reward network. As reward responsiveness of an individual is also influenced by endogenous opioid neurotransmission in key structures of the reward network, we hypothesized that opioid-induced behavioral analgesia would be predicted by trait reward responsiveness (RWR) and activity in parts of the reward circuitry to noxious stimulation at baseline before opioid infusion. These relationships have not been determined to date, yet could have translational relevance, as measures that better stratify patients as positive responders to therapeutic interventions are increasingly being sought.

We induced opioid analgesia to noxious heat stimuli using an i.v. infusion of the short-acting MOR agonist, remifentanil, in a large group of healthy volunteers. We measured the neuronal response [blood oxygen level dependent (BOLD) response] to these stimuli before the infusion and during the infusion using the noninvasive technique of functional magnetic resonance imaging (fMRI). We used the reward responsiveness subscale of Carver and White's behavioral inhibition system/behavioral activation system (BIS/BAS) scale (19) to measure the individual's response to rewarding stimuli.

Results

Twenty-five subjects (mean age, 30 y; age range, 21–46 y; 11 females) attended two visits where moderately painful heat stimuli were delivered via a contact thermode on the right forearm, as blocks of 10 stimuli before (preinfusion) and during a 40-min infusion of μ-opioid agonist (remifentanil) or saline (control visit). The main experimental design is previously published (20). The

Author contributions: V.W., R.R., and I.T. designed research; V.W., M.C.L., and R.R. performed research; V.W., Y.K., S.L., J.A., and I.T. analyzed data; and V.W., M.C.L., R.R., Y.K., S.L., J.A., and I.T. wrote the paper.

The authors declare no conflict of interest.

This article is a PNAS Direct Submission. H.L.F. is a guest editor invited by the Editorial Board.

Freely available online through the PNAS open access option.

[1]To whom correspondence should be addressed. E-mail: vishwani@fmrib.ox.ac.uk.

This article contains supporting information online at www.pnas.org/lookup/suppl/doi:10.1073/pnas.1120201109/-/DCSupplemental.

experimental design is outlined in Fig. S1. Remifentanil induced a significant reduction ($P < 0.01$) in heat pain intensity ratings (Fig. 1) and a significant increase in mental and physical sedation (Fig. S2). The increases in tranquility and sociability scores were not statistically significant. The opioid-induced changes in psychophysical variables were defined as [v opioid$_{(\text{infusion} - \text{preinfusion})}$] − [$v$ saline$_{(\text{infusion} - \text{preinfusion})}$], where v is the psychophysical variable. A negative value indicates a reduction. See *SI Results* for details of opioid-induced changes in mental and physical sedation, tranquility, sociability, and cardiorespiratory variables.

Main Psychophysical Finding. As hypothesized, the magnitude of behavioral analgesia correlated positively with trait RWR ($r = 0.61$; $P < 0.01$) (Fig. 1). To express opioid-induced behavioral analgesia as a positive value, we defined it as [v opioid$_{(\text{preinfusion} - \text{infusion})}$] − [$v$ saline$_{(\text{preinfusion} - \text{infusion})}$], where v is the pain intensity. This effect is driven by the remifentanil infusion and not by the saline infusion (Fig. S3).

The opioid-induced changes in sedation, tranquility, and sociability did not show a significant correlation with either opioid-induced behavioral analgesia or trait RWR.

We used a perception-locked stimulus in all subjects for both visits by adjusting the temperature of the contact-thermode stimulus to achieve a subjective rating of moderate pain. The stimulus temperature was kept constant between baseline and the subsequent remifentanil/saline block for an individual, but the temperature was not the same for every subject. However, there was no significant difference between the group mean temperatures used for the two visits. The mean temperature (±SD) used was 50.8 °C (±1.7) during the saline visit and 50.6 °C (±1.9) during the remifentanil visit. Importantly, there was no relationship between the temperature used and the magnitude of analgesia subsequently produced (Fig. S4).

BOLD Signal Change to Noxious Stimuli During the Preinfusion Period. There are no significant differences in the neuronal response (BOLD signal change) to noxious stimuli between the remifentanil and saline preinfusion periods anywhere in the brain. This is consistent with preinfusion period psychophysical data that show no difference between the two visits (*SI Results*).

The average neuronal response to noxious stimuli during the preinfusion period for each subject was generated by averaging the two preinfusion period functional scans. Using these maps in a model with a regressor for the analgesia score, we asked whether

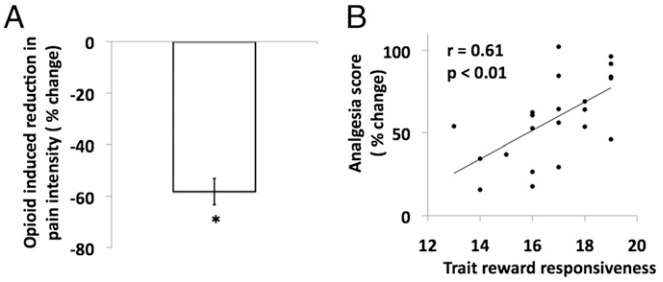

Fig. 1. Opioid-induced reduction in pain intensity and behavioral analgesia. (*A*) *Y* axis shows the mean opioid-induced reduction in pain intensity (percentage of change) of heat noxious stimuli. The opioid-induced reduction in pain intensity is defined as [v opioid$_{(\text{infusion} - \text{preinfusion})}$] − [$v$ saline$_{(\text{infusion} - \text{preinfusion})}$], where v is the pain intensity. Error bars indicate SEM (one-sample t test; $^*P < 0.01$). (*B*) Scatter plot of significant positive correlation ($r = 0.61$; $P = 0.002$) between the opioid-induced behavioral analgesia as percentage of change in pain intensity (y axis) and the trait reward responsivness score (x axis). To depict analgesia as a positive value, it is defined as [v opioid$_{(\text{preinfusion} - \text{infusion})}$] − [$v$ saline$_{(\text{preinfusion} - \text{infusion})}$], where v is pain intensity. Pearson's r and P values are shown in the scatter plot.

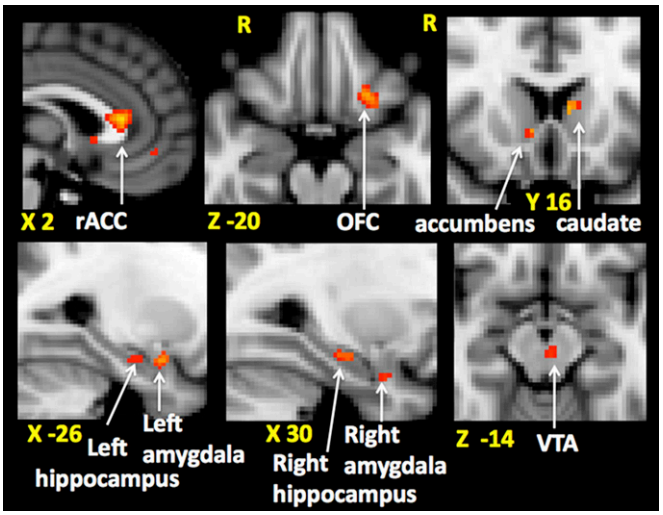

Fig. 2. Areas of the brain where preinfusion period neuronal response to noxious stimuli predict opioid-induced behavioral analgesia. Behavioral analgesia (percentage of change in pain intensity) is defined as [v opioid$_{(\text{preinfusion} - \text{infusion})}$] − [$v$ saline$_{(\text{preinfusion} - \text{infusion})}$], where v is pain intensity. Clusters of voxels in the rostral anterior cingulate cortex (rACC), left orbitofrontal cortex (OFC), right nucleus acumbens, left caudate (in the *Upper* row from *Left* to *Right*), left amygdala and hippocampus, right amygdala and hippocampus, ventral tegmental area (VTA), (*Lower* row, *Left* to *Right*) are shown. Montreal Neurological Institute coordinates are denoted in millimeters below each slice.

the magnitude of analgesia is predicted by the preinfusion period neuronal response anywhere in the brain (whole brain analysis) and in nine reward-processing areas of the brain (hypothesis-based directed searches). This revealed that the higher the preinfusion period brain activity to noxious stimuli in reward-related areas of the brain the greater the subsequent behavioral analgesia. These baseline, preinfusion active brain areas were: the left orbitofrontal cortex (OFC) and rostral anterior cingulate cortex (rACC) identified using whole brain analysis, bilateral hippocampi, bilateral amygdala, the left caudate, the right nucleus accumbens (NAc), and ventral tegmental area (VTA) (Fig. 2) identified using directed searches (masks shown in Fig. S5 and localization of VTA activity shown in Fig. S6). This relationship is illustrated with scatter plots in Fig. S7.

Further, we also found a positive correlation between the preinfusion period brain activity (extracted percentage of BOLD) from voxels that predicted behavioral analgesia and subjects' trait RWR scores. This relationship is statistically significant in all areas except for the VTA and left hippocampus (*SI Results*).

To determine whether any of these brain regions predict analgesia independent of that predicted from RWR, we performed a partial correlation between the brain activities identified at baseline as predictive of behavioral analgesia after accounting for RWR score. This revealed that the preinfusion period brain activity significantly predicted the behavioral analgesia score independent of RWR in the following brain areas: VTA ($r = 0.507$; $P = 0.016$), left caudate ($r = 0.563$; $P = 0.017$), left OFC ($r = 0.448$; $P = 0.037$), and rACC ($r = 0.505$; $P = 0.017$). By combining all brain regions identified at baseline as predictive of behavioral analgesia independent of RWR, the significance was $r = 0.571$; $P = 0.005$.

Opioid-Induced Changes in Neuronal Response to Noxious Stimuli. For each subject, the brain activity map representing the opioid-induced changes was generated using the functional scans obtained from the two preinfusion periods and the two infusion periods. Opioid-induced changes are defined as

[v opioid$_{(\text{preinfusion}-\text{infusion})}$] − [$v$ saline$_{(\text{preinfusion}-\text{infusion})}$], where v is the neuronal response evoked by noxious stimuli. These maps were used in a model containing a regressor for the group mean of the opioid-induced changes in brain activity and another regressor for the analgesia score. This identified brain areas with opioid-induced changes in activity and brain areas where the change in activity specifically correlated with the analgesia score. Using hypothesis-based directed searches we specifically asked whether nine reward-related brain regions that predicted the analgesia magnitude during the preinfusion period influenced the expression of behavioral analgesia during the infusion.

The opioid suppressed the neuronal response to noxious stimuli in bilateral insular, bilateral basal ganglia, and the anterior cingulate cortex (ACC) (whole brain analysis) (Fig. S8).

The more informative analysis exploring the relationship between opioid-induced neuronal response and opioid analgesic score revealed a significant positive correlation between the opioid-induced changes in brain activity and the magnitude of behavioral analgesia in the following areas: bilateral thalamus, periaqueductal gray (PAG) and rostral ventromedial medulla (RVM) using whole brain analysis (localization of RVM shown in Fig. S6), left hippocampus, and bilateral amygdala (Fig. 3) using directed searches (masks shown in Fig. S5). This relationship is illustrated with scatter plots in Fig. S9. Interestingly, the opioid-induced changes in brain activity from voxels in these areas failed to show a significant correlation with trait RWR (*SI Results*).

There was no significant correlation between the opioid-induced changes in brain activity and the magnitude of analgesia in the rACC, left OFC, left caudate nucleus, right NAc, and VTA, areas of the reward circuitry that predicted behavioral opioid analgesia in the preinfusion period. Rather it is possible that these areas drive brain activity changes during the opioid infusion within those specific brain regions whose opioid-induced change in neural activity does correlate with behavioral analgesia (i.e., bilateral amygdala, hippocampus, PAG, and RVM). To investigate this, we used the group mean maps of the opioid-induced changes in brain activity and a regressor for the neuronal (extracted percentage of BOLD) response to noxious stimuli during the preinfusion period from the voxels in the right NAc and VTA (key nuclei in the reward circuitry) that predicted the behavioral analgesia score. We limited our searches to the bilateral amygdala, left hippocampus, PAG, and RVM as they contributed to the expression of opioid analgesia in our study and are components of the descending pain modulatory system (DPMS) and reward circuitry (masks shown in Fig. S5). We found a significant positive correlation between the preinfusion period neuronal response to noxious stimuli in the VTA and the opioid-induced changes in the right amygdala, left hippocampus, and the RVM only (Fig. 4). The preinfusion period brain activity to noxious stimuli in the right NAc showed a significant positive correlation only with the opioid-induced changes in neural activity in the RVM.

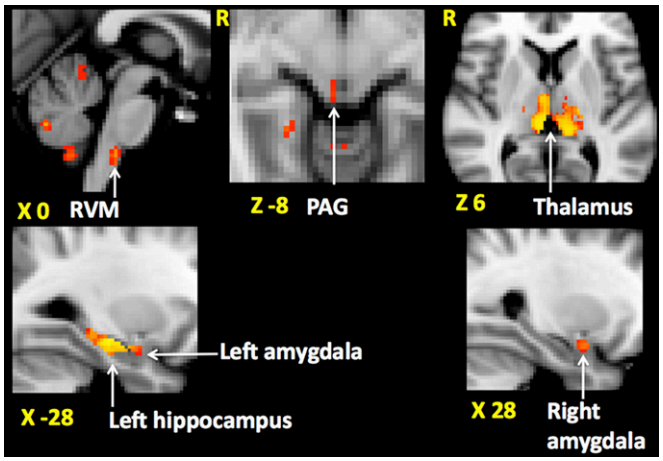

Fig. 3. Areas of the brain where opioid-induced changes in neuronal response to noxious stimuli show a significant positive correlation with opioid-induced behavioral analgesia. Opioid-induced changes in neuronal response and behavioral analgesia are defined as [v opioid$_{(\text{preinfusion}-\text{infusion})}$] − [$v$ saline$_{(\text{preinfusion}-\text{infusion})}$], where v is the neuronal response or the pain intensity of noxious stimuli. A positive value for the change in neuronal response indicates an opioid-induced reduction. A positive correlation means the higher the behavioral analgesia the higher the opioid-induced suppression of the neuronal response. Clusters of voxels in rostral ventromedial medulla (RVM), periaqueductal gray (PAG), bilateral thalamus (in the *Upper* row from *Left* to *Right*), left amygdala and hippocampus and the right amygdala (*Lower* row, *Left* to *Right*) are shown. Montreal Neurological Institute coordinates are denoted in millimeters below each slice.

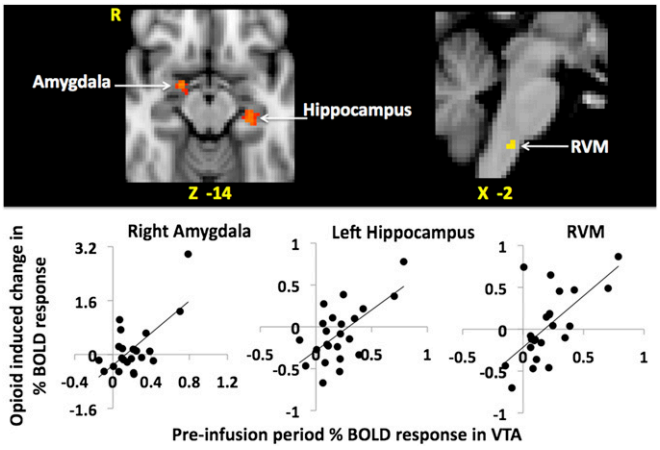

Fig. 4. Areas of the brain where preinfusion period neuronal response to noxious stimuli in the ventral tegmental area (VTA) show a significant positive correlation with opioid-induced changes in neuronal response to noxious stimuli. Opioid-induced changes in neuronal (percentage of BOLD) response are defined as [v opioid$_{(\text{preinfusion}-\text{infusion})}$] − [$v$ saline$_{(\text{preinfusion}-\text{infusion})}$], where v is the neuronal response to noxious stimuli. A positive value for the change in neuronal response indicates an opioid-induced reduction. A positive correlation means the higher the preinfusion period neuronal response in the VTA the higher the opioid-induced suppression of the neuronal response. Clusters of voxels in right amygdala, left hippocampus, and rostral ventromedial medulla (RVM) (in the *Upper* row from *Left* to *Right*), are shown. Montreal Neurological Institute coordinates are denoted in millimeters below each slice. The respective scatter plots below illustrates these relationships.

Discussion

To improve the understanding of factors contributing to the variability of the opioid analgesic response, we investigated the relationship between behavioral opioid analgesia and neural correlates of opioid-induced analgesia, trait RWR, and the responsiveness of the reward network to noxious stimuli at baseline as a likely predictive network.

Carver and White's RWR scale measures individual differences in sensitivity to reward signals and the ability to respond positively when exposed to such signals (19). We used this scale in our cohort of subjects and found that those individuals with high RWR score experienced a higher magnitude of behavioral opioid analgesia, in this instance the reward being the analgesia. Our imaging results show that the magnitude of this reward i.e., analgesia is predicted by the preinfusion period neuronal response to a noxious stimulus in areas of the left OFC, rACC, bilateral hippocampi, bilateral amygdala, the left caudate, the right NAc, and VTA: areas that play a role in reward processing (7). This neuronal response was higher in individuals with a high RWR score. Human opioid

receptor imaging studies indicate that several of these regions are components of the endogenous opioid system (14) and show increased activation in response to noxious stimuli (4) particularly in those individuals with higher scores on reward-related personality traits (21). Based on these findings, although our study is not a receptor imaging study, we believe that the neuronal response to noxious stimuli in a similar set of areas is reflecting the reactivity of the endogenous opioid neurotransmission. As exogenous opioids mediate behavioral analgesia via the endogenous opioid system (3) it is not surprising that the reactivity of this system is able to predict the magnitude of subsequent exogenous opioid-induced behavioral analgesia experienced by our subjects. As reward-related personality traits are underpinned by endogenous opioid neurotransmission, we believe that the RWR score in our subjects is a psychophysical measure of the reactivity of the areas of the endogenous opioid system that predicted opioid analgesia. Of these brain areas the baseline activity in the VTA, left caudate, rACC, and the left OFC predicted the behavioral analgesia score *beyond* RWR, illustrating the utility of fMRI rather than behaviorally based measures as potentially useful predictive metrics as has been shown in other domains (10).

Opioid-Induced Changes in Neuronal Response to Noxious Stimuli. In line with previous studies, the opioid induced a significant suppression of the neuronal response to noxious heat stimuli in many areas of the cerebral pain network (22, 23). As this result is derived from a group of low, medium, and high opioid analgesic responders, the threshold criterion will not necessarily show significant changes in all pain-related brain regions.

Therefore, to extract more meaningful results, we examined the relationship between the opioid-induced change in the neuronal response to noxious stimuli and the magnitude of behavioral analgesia. We observed a significant positive correlation between these two measures in areas of the DPMS, specifically the PAG, RVM, and amygdala. These areas of the DPMS receive nociceptive information from the periphery (24), contain MORs, and when activated by exogenous opioids contribute to opioid-induced behavioral analgesia (18, 25). The amygdala has direct projections to the PAG (26), which in turn projects to the RVM (27). PAG and RVM contain "on cells" and "off cells" (28, 29). In animals, on cells start firing while off cells stop firing in response to a noxious stimulus. Therefore, it is possible that the increased neuronal response to noxious stimuli in these areas observed in human imaging studies (30, 31) indicates the activity of the on cells. In our study, we define opioid-induced changes as $[v\ \text{opioid}_{(\text{preinfusion}-\text{infusion})}] - [v\ \text{saline}_{(\text{preinfusion}-\text{infusion})}]$, where v is the neuronal response to noxious stimuli. A positive value indicates the magnitude of the opioid-induced reduction of the neuronal response. This means that the *higher* the analgesia the *lower* the activation of these areas in response to noxious stimulation. We believe this to represent the reduced nociceptive input to these supraspinal sites by the opioid-induced inhibition of the nociceptive transmission at the spinal dorsal horn. This would be achieved by the direct inhibitory action of opioids on the dorsal horn nociceptive transmission (32) and the indirect inhibitory action of opioids via *activation* of the descending inhibitory pathways (disinhibition of the off cells) or via *suppression* of the descending facilitatory pathways (inhibition of the on cells) (27).

Although the preinfusion period neuronal response to noxious stimuli in areas of the reward circuitry such as the rACC, OFC, NAc, caudate nucleus, and the VTA predicted opioid-induced behavioral analgesia, the opioid-*induced* brain activity in these structures did not correlate with the behavioral opioid analgesia reflecting a dissociation. It is possible that these structures influence the expression of behavioral opioid analgesia indirectly via other areas of the reward circuitry such as the amygdala and the hippocampus. Animal studies show that dopamine neurons of the VTA contribute to opioid-induced analgesia (17) and send efferents to both the hippocampus and the amygdala (33, 34). In keeping with these anatomical and functional links, we found that the preinfusion period neuronal response of the VTA that predicted the subsequent behavioral analgesia also significantly predicted the opioid-induced changes in neuronal activity in the right amygdala and the left hippocampus, areas that were shown to influence the expression of behavioral analgesia in our study. A similar relationship between the NAc and the hippocampus and the amygdala was not strong enough to survive statistical corrections. This is most likely because the NAc influences these structures indirectly via the pallidum and the VTA (35). Areas such as the rACC, a key area of the endogenous opioid system, could also be influencing the expression of opioid analgesia via its well-known functional links with the PAG and the RVM (15, 36).

Role of the Amygdala and the Hippocampus in Opioid Analgesia. The hippocampus and the amygdala are components of the reward network with anatomical and functional links that regulate goal-directed behavior through the NAc (35). This functional congruity of the hippocampus, amygdala, and NAc is demonstrated in our results where the magnitude of a reward (behavioral opioid analgesia) is predicted by the neuronal response of these structures to an aversive stimulus.

Importantly, the opioid-induced changes in the brain activity in the amygdala and the hippocampus also show a significant positive correlation with the behavioral analgesia score, similar to that observed in the PAG and RVM. It is likely that the amygdala, rich in MORs, contributes to and influences the expression of behavioral opioid analgesia most probably via its connections with the PAG and RVM.

Based on preclinical studies, nociceptive processing in the hippocampus is thought to be intensity dependent (37). Consistent with these findings, human imaging studies have reported activation of the hippocampus in an intensity-dependent manner whether the change in perceived intensity of a noxious stimulus is due to increased stimulus intensity or anxiety (38, 39). Our finding that the higher the analgesia the higher the opioid-induced suppression of the neuronal response to noxious stimuli is in keeping with the intensity-dependent nature of nociceptive processing in the hippocampus.

Based on preclinical studies (16) it is also possible that in our subjects, opioids act directly on the hippocampus suppressing the neuronal response to noxious stimuli. Interestingly, the hippocampus contains neurons that are excited by noxious stimuli and neurons that are inhibited by noxious stimuli (40). Furthermore, pain and analgesic behaviors can both be produced by varying the frequency of the stimulating electrode placed in the hippocampus without changing the site of stimulation (41). This bidirectional response to nociceptive stimuli and the presence of endogenous opioid receptors make it possible for the hippocampus to perform a pain modulatory role similar to that of the amygdala, a structure that mediates exogenous opioid analgesia and has the ability to produce hyperalgesia or analgesia depending on the emotional context in which the nociceptive stimulus is perceived (42).

Conclusion

Our results reveal that individuals with high reward responsiveness, a personality trait dependent on the endogenous opioid neurotransmission, experience more exogenous opioid-induced behavioral analgesia. The magnitude of this reward i.e., analgesia, was best predicted by the neural activity in the endogenous opioid-rich regions of the brain reward circuitry. Emerging evidence suggests that MOR polymorphism could contribute to variability in behavioral opioid analgesia by introducing variability of the MOR responsiveness to exogenous opioids. However, there is also an urgent need for endophenotypes that are simpler measurable markers that link behavior and genetics that underpin such behavior (43). It is possible that trait RWR and the neuronal

response to noxious stimuli in the endogenous opioid-rich brain reward circuitry could be useful endophenotypes of behavioral opioid analgesia. As such, we have identified potentially useful measures to aid stratification of patients at baseline that are predictive of opioid-induced analgesia contributing to a personalized approach to opioid pharmacotherapy.

Methods

General details of the study methods are published elsewhere (20). The methods specific to the data presented here are given below and in *SI Methods*.

Study Procedure. Thirty-three healthy subjects were recruited after obtaining written informed consent. Of these, 25 subjects completed the study. See *SI Methods* for details of excluded subjects. This research was approved by the Oxfordshire Research Ethics Committee B of the National Research Ethics Services (NRES).

During the two scanning visits the same cohort of subjects received an infusion of remifentanil during one of the visits and a saline infusion during the other (balanced for order), separated by at least 1 wk. They received a remifentanil infusion at an effect site concentration of 2 ng mL^{-1} for 30 min using a target-controlled infusion (TCI) pump, which delivers the desired effect site concentration controlling for the effects of subject demographics (Fig. S4 shows lack of influence of demographics on analgesia score). Total duration of the infusion was 40 min allowing 10 min to reach the steady effect site concentration. The subjects completed the BIS/BAS scale before scanning on the first visit.

fMRI Scanning and Stimulation Paradigm. Functional imaging data were acquired using a 3T Varian-Siemens whole-body magnetic resonance scanner. See *SI Methods* for image acquisition details. Once the subject was in the scanner, we connected the infusion to an indwelling cannula in the left forearm and began physiological monitoring.

We used heat and punctate noxious stimuli. These were delivered separately in blocks of 10 stimuli before, during, and after the infusion with the heat stimulation blocks preceding the punctate stimulation blocks. The data from the postinfusion period and noxious punctate stimuli were used to investigate opioid withdrawal-induced hyperalgesia and are published elsewhere.

The temperature that delivered a moderately painful stimulus (5 on a numerical rating scale, NRS, where 0 corresponds to "no pain" and 10 to "severe pain") was selected for each subject for each visit with the subject in the scanner but before starting the experiment. The same temperature was used for all stimuli during that visit for the individual subject.

After obtaining preinfusion period mood scores, functional scans began while delivering the noxious stimulation block, each consisting of 10 stimuli over ~10 min. A visual analog scale (VAS) was used for recording perceived pain intensity of each stimulus. The infusion was commenced and the stimulation block was repeated during the infusion. Mood ratings were obtained before and after the stimulation block during the infusion period.

Analysis of Psychophysical Data. Paired two-tailed *t* tests were used for comparison of baseline data from the two visits. A one-sample two-tailed *t* test was performed to evaluate whether the distribution of the opioid infusion-induced effects were significantly different from a mean of zero. For data that were nonnormally distributed, we used the Wilcoxon signed rank test.

Analysis of fMRI Data. fMRI analyses of the heat functional scans were performed using FEAT (FMRI Expert Analysis Tool) version 5.98, part of the Oxford Centre for Functional Magnetic Resonance Imaging of the Brain software library; www.fmrib.ox.ac.uk/fsl (FSL). Statistical images were generated to identify significant brain activity evoked by noxious stimuli in each functional scan. These were then analyzed at higher levels to generate the necessary group statistical maps. For whole brain analyses we used mixed effects analysis and a cluster-based correction for multiple comparisons (Z score >2.3; $P < 0.05$). Where appropriate, we performed a priori hypothesis-driven directed searches using small volume correction with nonparametric permutation testing (5,000 permutations) (44) and threshold free cluster enhanced (TFCE) correction for multiple comparisons at $P < 0.05$ (45). All our directed searches were thresholded individually to yield a 5% false positive rate for each of the searches.

To illustrate significant results from image analyses, we extracted the percentage of BOLD response. To define brain structures for small volume corrections, we used the Harvard Oxford Cortical and Subcortical Structural Atlas (http://www.fmrib.ox.ac.uk/fsl/data/atlas-descriptions.html). For correct identification of brainstem areas, we used the Duvernoy Brainstem Atlas (46). Details of how these areas were identified are in *SI Methods*.

ACKNOWLEDGMENTS. This work was supported by Grants from the Medical Research Council of Great Britain and Northern Ireland, the National Institute for Health Research Oxford Biomedical Research Centre, and the Wellcome Trust (Oxford Centre for Functional MRI of the Brain) (to M.C.L., V.W., and I.T.).

1. Anonymous; Expert Working Group of the European Association for Palliative Care (1996) Morphine in cancer pain: Modes of administration. *BMJ* 312:823–826.
2. Lötsch J, Geisslinger G (2005) Are mu-opioid receptor polymorphisms important for clinical opioid therapy? *Trends Mol Med* 11:82–89.
3. Dickenson AH, Kieffer B (2006) Opiates: Basic mechanisms. *Wall and Melzack's Textbook of Pain*, eds McMahon SB, Koltzenburg M (Churchill Livingstone, New York), 5th Ed.
4. Zubieta JK, et al. (2001) Regional mu opioid receptor regulation of sensory and affective dimensions of pain. *Science* 293:311–315.
5. Barbano MF, Cador M (2006) Differential regulation of the consummatory, motivational and anticipatory aspects of feeding behavior by dopaminergic and opioidergic drugs. *Neuropsychopharmacology* 31:1371–1381.
6. Schreckenberger M, et al. (2008) Opioid receptor PET reveals the psychobiologic correlates of reward processing. *J Nucl Med* 49:1257–1261.
7. Haber SN, Knutson B (2010) The reward circuit: Linking primate anatomy and human imaging. *Neuropsychopharmacology* 35(1):4–26.
8. D'Ardenne K, McClure SM, Nystrom LE, Cohen JD (2008) BOLD responses reflecting dopaminergic signals in the human ventral tegmental area. *Science* 319:1264–1267.
9. Gottfried JA, O'Doherty J, Dolan RJ (2003) Encoding predictive reward value in human amygdala and orbitofrontal cortex. *Science* 301:1104–1107.
10. Knutson B, Rick S, Wimmer GE, Prelec D, Loewenstein G (2007) Neural predictors of purchases. *Neuron* 53:147–156.
11. Yacubian J, et al. (2007) Subregions of the ventral striatum show preferential coding of reward magnitude and probability. *Neuroimage* 38:557–563.
12. Scott DJ, et al. (2007) Individual differences in reward responding explain placebo-induced expectations and effects. *Neuron* 55:325–336.
13. Baliki MN, Geha PY, Fields HL, Apkarian AV (2010) Predicting value of pain and analgesia: Nucleus accumbens response to noxious stimuli changes in the presence of chronic pain. *Neuron* 66:149–160.
14. Jones AK, et al. (1991) In vivo distribution of opioid receptors in man in relation to the cortical projections of the medial and lateral pain systems measured with positron emission tomography. *Neurosci Lett* 126:25–28.
15. Petrovic P, Kalso E, Petersson KM, Ingvar M (2002) Placebo and opioid analgesia—imaging a shared neuronal network. *Science* 295:1737–1740.
16. Favaroni Mendes LA, Menescal-de-Oliveira L (2008) Role of cholinergic, opioidergic and GABAergic neurotransmission of the dorsal hippocampus in the modulation of nociception in guinea pigs. *Life Sci* 83:644–650.
17. Franklin KB (1989) Analgesia and the neural substrate of reward. *Neurosci Biobehav Rev* 13:149–154.
18. McGaraughty S, Heinricher MM (2002) Microinjection of morphine into various amygdaloid nuclei differentially affects nociceptive responsiveness and RVM neuronal activity. *Pain* 96:153–162.
19. Carver C (1994) Behavioral inhibition, behavioral activation, and affective responses to impending reward and punishment: The BIS/BAS scale. *J Pers Soc Psychol* 67:319–333.
20. Wanigasekera V, Lee MC, Rogers R, Hu P, Tracey I (2011) Neural correlates of an injury-free model of central sensitization induced by opioid withdrawal in humans. *J Neurosci* 31:2835–2842.
21. Love TM, Stohler CS, Zubieta JK (2009) Positron emission tomography measures of endogenous opioid neurotransmission and impulsiveness traits in humans. *Arch Gen Psychiatry* 66:1124–1134.
22. Wise RG, Williams P, Tracey I (2004) Using fMRI to quantify the time dependence of remifentanil analgesia in the human brain. *Neuropsychopharmacology* 29:626–635.
23. Tracey I, Mantyh PW (2007) The cerebral signature for pain perception and its modulation. *Neuron* 55:377–391.
24. Gauriau C, Bernard JF (2002) Pain pathways and parabrachial circuits in the rat. *Exp Physiol* 87:251–258.
25. Jones SL, Gebhart GF (1988) Inhibition of spinal nociceptive transmission from the midbrain, pons and medulla in the rat: Activation of descending inhibition by morphine, glutamate and electrical stimulation. *Brain Res* 460:281–296.
26. Rizvi TA, Ennis M, Behbehani MM, Shipley MT (1991) Connections between the central nucleus of the amygdala and the midbrain periaqueductal gray: Topography and reciprocity. *J Comp Neurol* 303:121–131.
27. Fields H (2004) State-dependent opioid control of pain. *Nat Rev Neurosci* 5:565–575.
28. Fields HL, Bry J, Hentall I, Zorman G (1983) The activity of neurons in the rostral medulla of the rat during withdrawal from noxious heat. *J Neurosci* 3:2545–2552.
29. Heinricher MM, Cheng ZF, Fields HL (1987) Evidence for two classes of nociceptive modulating neurons in the periaqueductal gray. *J Neurosci* 7:271–278.
30. Dunckley P, et al. (2005) A comparison of visceral and somatic pain processing in the human brainstem using functional magnetic resonance imaging. *J Neurosci* 25:7333–7341.

31. Gwilym SE, et al. (2009) Psychophysical and functional imaging evidence supporting the presence of central sensitization in a cohort of osteoarthritis patients. *Arthritis Rheum* 61:1226–1234.
32. Glaum SR, Miller RJ, Hammond DL (1994) Inhibitory actions of delta 1-, delta 2-, and mu-opioid receptor agonists on excitatory transmission in lamina II neurons of adult rat spinal cord. *J Neurosci* 14:4965–4971.
33. Gasbarri A, Verney C, Innocenzi R, Campana E, Pacitti C (1994) Mesolimbic dopaminergic neurons innervating the hippocampal formation in the rat: A combined retrograde tracing and immunohistochemical study. *Brain Res* 668:71–79.
34. Hasue RH, Shammah-Lagnado SJ (2002) Origin of the dopaminergic innervation of the central extended amygdala and accumbens shell: A combined retrograde tracing and immunohistochemical study in the rat. *J Comp Neurol* 454:15–33.
35. Sesack SR, Grace AA (2010) Cortico-basal ganglia reward network: Microcircuitry. *Neuropsychopharmacology* 35:27–47.
36. Kong J, Tu PC, Zyloney C, Su TP (2010) Intrinsic functional connectivity of the periaqueductal gray, a resting fMRI study. *Behav Brain Res* 211:215–219.
37. Khanna S (2006) Nociceptive processing in the hippocampus and entorhinal cortex, neurophysiology and pharmacology. *Encyclopedia of Pain*, eds Schmidt RR, Willis WD (Springer, New York), pp 1369–1374.
38. Derbyshire SW, et al. (1997) Pain processing during three levels of noxious stimulation produces differential patterns of central activity. *Pain* 73:431–445.
39. Ploghaus A, et al. (2001) Exacerbation of pain by anxiety is associated with activity in a hippocampal network. *J Neurosci* 21:9896–9903.
40. Yang XF, Xiao Y, Xu MY (2008) Both endogenous and exogenous ACh plays antinociceptive role in the hippocampus CA1 of rats. *J Neural Transm* 115:1–6.
41. Lico MC, Hoffmann A, Covian MR (1974) Influence of some limbic structures upon somatic and autonomic manifestations of pain. *Physiol Behav* 12:805–811.
42. Neugebauer V, Li W, Bird GC, Han JS (2004) The amygdala and persistent pain. *Neuroscientist* 10:221–234.
43. Tracey I (2011) Can neuroimaging studies identify pain endophenotypes in humans? *Nat Rev Neurol* 7:173–181.
44. Nichols TE, Holmes AP (2002) Nonparametric permutation tests for functional neuroimaging: A primer with examples. *Hum Brain Mapp* 15:1–25.
45. Smith SM, Nichols TE (2009) Threshold-free cluster enhancement: Addressing problems of smoothing, threshold dependence and localisation in cluster inference. *Neuroimage* 44:83–98.
46. Naidich TP, et al. (2009) *Duvernoy's Atlas of the Human Brain Stem and Cerebellum* (Springer, New York).

Supporting Information

Wanigasekera et al. 10.1073/pnas.1120201109

SI Methods

General details of study methods of this experiment have already been published (1). A brief outline of general methods and a detailed account of the methods specific to the data presented in this manuscript are given below. Experimental design is outlined in Fig. S1.

Subjects. The Oxfordshire research ethics committee approved the study and subjects gave written informed consent. Thirty-three healthy subjects (American Society of Anesthesiologists physical status I) were recruited. Of these, 25 subjects (mean age, 30 y; age range, 21–46 y; 11 females) completed the study. Seven subjects were excluded during the screening visit, which was performed to ensure that the subjects tolerated an i.v. infusion of remifentanil (short acting μ-opioid agonist) and the study procedures. One subject failed to attend the subsequent scanning visits.

Study Design and Drug Infusion. For the two scanning visits, subjects received an infusion of remifentanil during one of the visits and a saline infusion during the other (balanced for order), separated by at least 1 wk. The subjects were blinded to the treatment. They fasted for 6 h before commencing the i.v. infusion. Remifentanil was delivered via an indwelling i.v. cannula inserted into the left forearm using a target controlled infusion (TCI) pump to achieve a steady state effect site concentration of 2 ng mL^{-1} for 30 min (2). We used a TCI pump to achieve an equivalent effect site concentration in all subjects during the steady state irrespective of subject demographics. The TCI pump achieves this by selecting the appropriate infusion rate based on the subject demographics to reach the set target effect site concentration. In this way, we minimize the influence of subject demographics on the remifentanil-induced effects (Fig. S4) by delivering a consistent effect site concentration (in this instance, 2 ng/mL) in all subjects during the steady state irrespective of subject demographics.

Total duration of the infusion was 40 min, allowing 10 min to reach the steady-state effect site concentration. Infusion was connected and monitoring was commenced after placing the subject in the scanner. To ensure subject safety throughout the experiment, we monitored the pulse rate, blood oxygen saturation (SpO2), respiratory rate, and end-tidal carbon dioxide partial pressures ($P_{ET}CO_2$) via nasal cannulae (Salter Labs). Oxygen 1–2 L/min was delivered via the nasal cannulae.

We delivered noxious stimuli while obtaining functional scans, assessed the mood levels, and gathered physiological data before (preinfusion period), during, and after the infusion. We used heat and punctate noxious stimuli. These were delivered separately in blocks of 10 stimuli before, during, and after the infusion with the heat stimulation blocks preceding the punctate stimulation blocks.

The data from the postinfusion period and noxious punctate stimuli were used to investigate opioid withdrawal-induced hyperalgesia and are published elsewhere (1).

Noxious Heat Stimulation. The heat stimuli were delivered using an in-house developed thermal resistor with a fast rise time (30° rise in 0.8 s) to deliver noxious heat stimuli via a thermode (3) attached to the medial–volar aspect of the proximal right forearm. The temperature delivered was selected for each subject for each visit with the subject in the scanner but before starting the experiment. By adjusting the temperature of the thermode, we identified a temperature that delivered a noxious stimulus that the subject perceived as moderately painful [5 on a numerical rating scale (NRS) where 0 corresponds to "no pain" and 10 to "severe pain"]. The same temperature was used for all heat stimuli during that visit for the individual volunteer. Ten such stimuli (each lasting for 3 s) were delivered 55–68 s apart before, during, and after the infusion. The intensity of each stimulus as experienced at the time of the noxious stimulus was recorded ∼15 s after the stimulus using a visual analog scale (VAS) displayed on a computer screen where the anchors were "no pain" and "severe pain."

Mood Scale. We tracked the level of tranquility, sociability, mental sedation, and physical sedation using the 16-item Bond-Lader mood scale (4). These were recorded during the preinfusion period, during the infusion period, and during the withdrawal period (∼20 min after stopping the infusion). The mood during the infusion was measured on reaching steady state just before starting the noxious stimulation block and at the end of the stimulation block just before stopping the infusion. The mood during the infusion was considered as the average of these two measurements.

Assessment of Reward Responsiveness Personality Trait. We used Carver and White's behavioral inhibition system (BIS)/behavioral activation system (BAS) scale (5), which characterizes individual personalities in terms of their response to aversive and rewarding stimuli. The BIS scale consists of items referencing to a punishing event. The BAS scale has three subscales: reward responsiveness (RWR), drive, and fun seeking. These have items focusing on positive responses to the experience or anticipation of a reward (RWR), relating to persistent pursuit of desired goals (drive), and reflecting the desire for new rewards and a willingness to approach a potentially rewarding event impulsively (fun seeking). These personality traits are underpinned by endogenous neurotransmitters such as dopamine (6), norepinephrine (7), serotonin (8), and opioids (9). The subscales used in these studies are from Cloniger's tridimentional personality questionnaire that has been validated against the BIS/BAS scale. Although these neurotransmitter systems interact with each other, we felt that it is important to assess the subscales differently as they measure different aspects of the behavioral activation system. This also makes the total BAS scale inappropriate to study a specific aspect of the behavioral activation system. Because we were examining an individual's response to a reward, in this instance, opioid-induced analgesia, we used the RWR subscale.

The subjects completed this questionnaire during the first scanning visit before any study intervention.

fMRI Data Acquisition. Functional imaging data were acquired using a 3T Varian-Siemens whole-body magnetic resonance scanner. We used a head-only gradient coil with a birdcage radiofrequency coil for pulse transmission and signal reception. A whole-brain (including the midbrain, pons, rostralmost medulla, and cerebellum) T2*-sensitive gradient echo-planar imaging (EPI) sequence with the following parameters was used: 3-s repetition time (TR), 30-ms echo time (TE), 0.5494-ms dwell time, 42 contiguous 3.5-mm-thick slices, field of view (FOV) 224 × 224 mm, and matrix 64 × 64. Functional scans acquired during the heat stimulation block consisted of 210 volumes. The first four volumes were discarded to permit equilibration of the blood oxygen level dependent (BOLD) signal. Fieldmaps were obtained using a symmetric-asymmetric spin-echo sequence after the preinfusion period functional scans. A T1 weighted structural (1 mm^3 voxel) image was acquired for the registration of statistical activation maps to the standard stereotactic space [Montreal Neurological Institute (MNI), 152 template].

Analysis of Psychophysical Data. Twenty-three complete datasets were available for analysis. D'Agostino and Pearson's omnibus normality test was used to examine the distribution of psychophysical data. For normally distributed data, the paired two-tailed t test was used for comparison of preinfusion period data from the two visits. A one-sample two-tailed t test was performed to evaluate whether the distribution of the opioid infusion-induced effects were significantly different from a mean of zero. For data that were nonnormally distributed, we used the Wilcoxon signed rank test.

Detection of differences in preinfusion period data. We tested for significant differences between the two visits in the following preinfusion period data: temperatures used, noxious stimulus intensity, the four aspects of the mood scale, and the four cardiorespiratory variables.

Detection of opioid-induced changes in psychophysical data. The opioid infusion induced effect for a given set of psychophysical variables (v) was defined by [v opioid$_{(\text{infusion}-\text{preinfusion})}$] − [$v$ saline$_{(\text{infusion}-\text{preinfusion})}$]. Subtracting the preinfusion period values from the infusion period values accounts for any preinfusion period differences between the visits. Subtracting the differences in the saline visit from those in the opioid visit accounts for the effect of time.

A negative value for an opioid infusion-induced effect indicates a reduction, whereas a positive value indicates an increase. To depict opioid-induced behavioral analgesia as a positive value, we defined it as [v opioid$_{(\text{preinfusion}-\text{infusion})}$] − [$v$ saline$_{(\text{basleine}-\text{infusion})}$], where v is pain intensity.

Correlation analysis. To test our hypothesis, we performed a correlation analysis between the trait reward responsiveness and the opioid-induced analgesia. We also performed a correlation analysis between opioid-induced behavioral analgesia and the opioid-induced mood changes. We assessed this relationship because mood and pain are known to influence each other (10). Furthermore, opioids not only result in analgesia but also in mood changes.

As we had a perception-matched stimulus for each subject during each visit, a change in nociceptive input between sessions and between subjects potentially can occur. Therefore, to assess the influence of temperature used on behavioral opioid analgesia, we performed a correlation analysis between these two parameters.

To confirm that we had minimized the influence of subject demographics on the remifentanil-induced behavioral analgesia by using a TCI pump to deliver the remifentanil, we performed correlation analyses between the analgesia score and subject demographics.

Analysis of fMRI Data. fMRI analyses were performed using FEAT (FMRI Expert Analysis Tool) version 5.98, part of the Oxford Centre for Functional Magnetic Resonance Imaging of the Brain software library (FSL); www.fmrib.ox.ac.uk/fsl. Preprocessing steps included motion correction (11), field-map correction of EPI distortion (12), removal of nonbrain voxels (13), spatial smoothing using a Gaussian kernel of the full width at half maximum 5-mm grand-mean intensity normalization of the entire 4D dataset by a single multiplicative factor and highpass temporal filtering with a cutoff of 100 s. Time-series statistical analysis was performed with local autocorrelation correction (14).

First-level analysis. Statistical analysis was performed for each of the functional scans for individual subjects using a general linear modeling approach. The input stimulus functions defined for the noxious stimuli and the rating tasks were convolved with the gamma hemodynamic function (mean lag, 6 s; full width at half height, 6 s) to yield regressors for the general linear model that described the BOLD activity in the functional scans. The estimated motion parameters for each subject were included as nuisance regressors. These analyses generated the parameter estimates (PEs) for the regressors that described the BOLD activity evoked by noxious stimuli for each stimulation block. Registration of functional images to each subject's high resolution T_1 scan, and then to the MNI standard brain was carried out using FLIRT (15).

Higher-level analysis. For all voxelwise brain analyses, we used mixed effects analysis (16) and a cluster-based correction for familywise error rate (FWR) (Z score >2.3; FWR $P < 0.05$). For hypothesis-driven searches, we performed a small volume correction using nonparametric permutation testing (5,000 permutations) (17) and threshold free cluster enhanced (TFCE) FWR correction at $P < 0.05$ (18). For small volume corrections (directed searches), regions were defined using the Harvard Oxford Cortical and Subcortical Structural Atlas (http://www.fmrib.ox.ac.uk/fsl/data/atlas-descriptions.html), which is a probabilistic population-based atlas. Only voxels estimated at greater than 50% probability of being in the structure were included in the region. For defining correct identification of brainstem areas, we used the Duvernoy Brainstem Atlas (19) because an automated detailed brainstem atlas is not available.

We used Featquery (http://fsl.fmrib.ox.ac.uk/fsl/fslwiki/FEAT/UserGuide#Featquery_output) for extraction of percentage of BOLD signal change evoked by the task from the significantly active voxels within an anatomical area. When extracting data from the brainstem structures, we used the Duvernoy Brainstem Atlas for correct identification of anatomical areas in the brainstem.

Using a voxelwise brain analysis and a paired test, we first searched for differences in brain activity evoked by noxious stimuli in the preinfusion periods between the two visits for the whole group.

Identifying areas of the brain where the preinfusion period neuronal response to noxious stimuli predicts the magnitude of opioid behavioral analgesia. The two preinfusion period statistical maps of each subject generated at the first-level analysis were entered into a second-level analysis with fixed effects to produce a statistical map that represented the average neuronal response to noxious stimuli during the preinfusion period for an individual subject. Using these maps, we next performed a voxelwise brain analysis (mixed effects analysis and a cluster-based correction for multiple comparisons: Z score >2.3; FWR $P < 0.05$) at the third level using a model containing a regressor for the group mean and another regressor with the opioid-induced behavioral analgesia score.

We also performed small volume corrections (nonparametric permutation testing and TFCE FWR correction at $P < 0.05$) to examine this relationship using nine directed searches in the key reward processing areas of the brain namely the bilateral nucleus accumbens (NAc), caudate, amygdala, hippocampus, and the mesencephalic tegmentum. (See Fig. S5 for the masks used.) The mesencephalic tegmentum was used for searching for activity in the ventral tegmental area (VTA). In this mask we included the area of the mesencephalon between a line drawn ventral to the aqueduct separating the tectum from the tegmentum, and a line drawn ventral to the substantia nigra separating the tegmentum from the white matter tracts.

To illustrate any significant relationships identified by these image analyses we extracted the percentage of BOLD signal response from the voxels in relevant areas. We then plotted these against the opioid-induced behavioral analgesia score.

To examine the relationship between the preinfusion period percentage of BOLD signal response to noxious stimuli from these voxels and the reward responsiveness score we performed a correlation analysis (Pearson's r) between these two variables.

Identifying areas with opioid-induced changes in neuronal response to noxious stimuli. For each subject, in a second level analysis using fixed effects we generated a statistical map representing the opioid infusion-induced changes in the neuronal response to noxious stimuli. For this analysis we used the outputs generated by the first-level analyses from the functional scans of the two preinfusion periods and the two infusion periods. We defined the opioid-induced changes in the neuronal response to noxious stimuli as

$[v\ \text{opioid}_{(\text{preinfusion}-\text{infusion})}] - [v\ \text{saline}_{(\text{preinfusion}-\text{infusion})}]$, where v is the BOLD response evoked by noxious stimuli. A positive value indicates the magnitude of the opioid-induced reduction of the neuronal response to noxious stimuli. This is the same method used for defining opioid-induced behavioral analgeisa as described previously.

Using these maps, we next performed a voxelwise analysis (mixed effects analysis and a cluster-based correction for multiple comparisons; Z score >2.3, FWR $P < 0.05$) at the third level using a model containing a regressor for the group mean of the opioid-induced changes in the neuronal response to noxious stimuli and another regressor with the opioid-induced behavioral analgesia score.

This would specifically identify areas of the brain with opioid-induced changes in neuronal response to noxious stimuli that correlated with the magnitude of the behavioral analgesia score. These would be areas of the brain that are implicated in mediating opioid-induced behavioral analgesia including the structures of the descending pain modulatory system (DPMS).

We used a small volume correction (nonparametric permutation testing and TFCE FWR correction at $P < 0.05$) to study this relationship in areas of the reward circuitry where the neuronal response to noxious stimuli during the preinfusion period predicted the magnitude of opioid-induced analgesia. These were the rostral anterior cingulate cortex (rACC), left orbitofrontal cortex (OFC), right and left amygdala, right and left hippocampus, right accumbens, left caudate, and the mesencephalic tegmentum. Clearly if these structures/areas predicted the behavioral analgesia at baseline, then there is a strong possibility that they could play a role in the opioid-induced response (masks shown in Fig. S5). The masks of the rACC area and left OFC are from the cluster of voxels with preinfusion period brain activity that significantly predicted behavioral analgesia. We used this method because the rACC is not defined in standard atlases and the OFC is a large area with functional diversity (20).

To illustrate any significant relationships identified by these image analyses we extracted the percentage of BOLD response from the voxels in relevant areas. Then we derived the opioid-induced change in percentage of BOLD response and plotted it against the opioid-induced behavioral analgesia score.

To examine the relationship between the opioid-induced changes in percentage of BOLD response to noxious stimuli from these voxels (voxels that showed a significant relationship in the above image analyses) and the reward responsiveness score we performed a correlation analysis (Pearson's r) between these two variables.

To examine the role of the key nuclei in the reward circuitry with preinfusion period brain activity that predicted subsequent behavioral analgesia, namely, the right NAc and the VTA, we performed another analysis. For this we used the group mean maps of the opioid-induced changes in brain activity and a regressor for the neuronal (extracted percentage of BOLD) response to noxious stimuli during the preinfusion period from the voxels in the right NAc and VTA (key nuclei in the reward circuitry) that predicted the behavioral analgesia score. For this analysis we limited the search to bilateral amygdala, left hippocampus, periaqueductal gray (PAG), and rostral ventromedial medulla (RVM), as they contributed to the expression of opioid analgesia in our study and are components of the DPMS as well as reward circuitry (masks shown in Fig. S5).

SI Results

Of the 33 subjects recruited, 25 (mean age, 30 y; age range, 21–46 y; 11 females) completed a two-way crossover study. Of the eight subjects not scanned, five were excluded due to opioid-induced nausea during the screening visit, one subject was intolerant of the i.v. cannula, one subject was claustrophobic in the scanner, and one subject failed to attend both scanner sessions.

Datasets from 23 of the 25 subjects were analyzed. Data from one subject was excluded because the average threshold temperature of 41 °C was well below the nociceptive threshold and more than two SDs lower than the rest of the subjects. The data from the other subject were excluded due to motion artifacts and incorrect timing in the functional scans due to equipment malfunction.

Preinfusion Period: Psychophysical Data. There are no significant differences ($P > 0.05$) in group means of the following preinfusion period psychophysical variables between the two visits: temperature required to elicit moderately painful stimuli, perceived intensity of the heat noxious stimulus, mood (tranquility, sociability, mental sedation, and physical sedation), or cardiorespiratory variables [end-tidal carbon dioxide partial pressures ($P_{ET}CO_2$), respiratory rate, blood oxygen saturation (SpO2), and pulse rate].

Group mean value (±SD) of these preinfusion period variables during the saline visit for the temperature used was 50.8 °C (±1.7), heat pain intensity (visual analog scale, VAS) was 5.1 (±0.8), tranquility (VAS) was 7.5 (±1.5), sociability (VAS) was 7.0 (±1.4), mental sedation (VAS) was 3.1 (±1.8), physical sedation (VAS) was 2.9 (±1.3), $P_{ET}CO_2$ (in millimeters of mercury) was 41.2 (±4.3), respiratory rate (breaths per minute) was 15 (±3), SpO2 (percentage) was 98.4 (±0.8), and pulse rate (beats per minute) was 58 (±7).

Group mean value (±SD) of these preinfusion period variables during the remifentanil visit for the temperature used was 50.6 °C (±1.9), heat pain intensity (VAS) was 5.1 (±1.0), tranquility (VAS) was 7.5 (±1.6), sociability (VAS) was 7.1 (±1.5), mental sedation (VAS) was 2.9 (±2.1), physical sedation (VAS) was 2.8 (±1.6), $P_{ET}CO_2$ (in millimeters of mercury) was 40.6 (±4.0), respiratory rate (breaths per minute) was 15 (±3), SpO2 (%) was 98.7 (±0.7), and pulse rate (beats per minute) was 58 (±8).

Preinfusion Period: fMRI Data. There are no significant differences in the neuronal response to noxious stimuli between the remifentanil and saline preinfusion periods anywhere in the brain. This is consistent with preinfusion period psychophysical data that show no differences between the two visits.

There is a positive correlation between the preinfusion period brain activity (extracted percentage of BOLD) from voxels in reward regions that predicted behavioral analgesia and subjects' trait reward responsiveness (RWR) scores. This relationship is statistically significant in the following areas: left OFC ($r = 0.5$; $P = 0.01$), rACC ($r = 0.44$; $P = 0.04$), right accumbens ($r = 0.54$; $P = 0.01$); left caudate ($r = 0.46$; $P = 0.03$); right amygdala ($r = 0.42$; $P = 0.045$); left amygdala ($r = 0.55$; $P = 0.01$), and right hippocampus ($r = 0.44$; $P = 0.04$). This relationship in the VTA ($r = 0.37$; $P = 0.08$) and left hippocampus ($r = 0.32$; $P = 0.13$) failed to reach statistical significance.

Opioid-Induced Changes: Psychophysical Data. Remifentanil at an effect site concentration of 2 ng mL^{-1} induced the following mood changes: significant increases ($P < 0.01$) in mental and physical sedation and nonsignificant increases in tranquility and sociability (Fig. S2). These opioid-induced changes do not show a significant correlation with either the opioid-induced behavioral analgesia or the RWR trait ($P \geq 0.16$).

There were no significant influences of temperature used nor subject demographics on behavioral opioid-induced analgesia (Fig. S4).

As anticipated the opioid infusion induces a statistically significant reduction in the respiratory rate ($P < 0.01$), a higher $P_{ET}CO_2$ ($P < 0.01$) and a reduction in SpO_2 ($P < 0.05$). The mean changes (±SD) for respiratory rate is 3.7 (±3) breaths/min, $P_{ET}CO_2$ is 5.5 (±4.2) mmHg, and SpO_2 is 0.5 (±0.8) %. These changes are clinically insignificant and did not compromise

the safety of the subject. There are no significant opioid-induced changes in the pulse rate.

Opioid-Induced Changes: fMRI Data. The opioid-induced changes in neuronal (extracted percentage of BOLD) response to noxious stimuli in voxels that showed a significant correlation with the magnitude of the behavioral opioid analgesia failed to show a significant correlation with trait RWR. The correlation coefficient of this relationship in the thalami is 0.33 ($P = 0.13$), in PAG, 0.03 ($P = 0.89$), in RVM, 0.28 ($P = 0.20$), in left hippocampus, 0.35 ($P = 0.10$), in right amygdala, 0.33 ($P = 0.12$), and in left amygdala, 0.37 ($P = 0.10$).

1. Wanigasekera V, Lee MC, Rogers R, Hu P, Tracey I (2011) Neural correlates of an injury-free model of central sensitization induced by opioid withdrawal in humans. *J Neurosci* 31:2835–2842.
2. Minto CF, Schnider TW, Shafer SL (1997) Pharmacokinetics and pharmacodynamics of remifentanil. II. Model application. *Anesthesiology* 86:24–33.
3. Wise RG, et al. (2002) Combining fMRI with a pharmacokinetic model to determine which brain areas activated by painful stimulation are specifically modulated by remifentanil. *Neuroimage* 16:999–1014.
4. Bond AJ, James DC, Lader MH (1974) Physiological and psychological measures in anxious patients. *Psychol Med* 4:364–373.
5. Carver C (1994) Behavioral inhibition, behavioral activation, and affective responses to impending reward and punishment: The BIS/BAS scale. *J Pers Soc Psychol* 67: 319–333.
6. Zald DH, et al. (2008) Midbrain dopamine receptor availability is inversely associated with novelty-seeking traits in humans. *J Neurosci* 28:14372–14378.
7. Garvey MJ, Noyes R, Jr., Cook B, Blum N (1996) Preliminary confirmation of the proposed link between reward-dependence traits and norepinephrine. *Psychiatry Res* 65:61–64.
8. Hansenne M, Ansseau M (1999) Harm avoidance and serotonin. *Biol Psychol* 51:77–81.
9. Schreckenberger M, et al. (2008) Opioid receptor PET reveals the psychobiologic correlates of reward processing. *J Nucl Med* 49:1257–1261.
10. Villemure C, Bushnell MC (2009) Mood influences supraspinal pain processing separately from attention. *J Neurosci* 29:705–715.
11. Jenkinson M, Bannister P, Brady M, Smith S (2002) Improved optimization for the robust and accurate linear registration and motion correction of brain images. *Neuroimage* 17:825–841.
12. Jenkinson M (2003) Fast, automated, N-dimensional phase-unwrapping algorithm. *Magn Reson Med* 49:193–197.
13. Smith SM (2002) Fast robust automated brain extraction. *Hum Brain Mapp* 17: 143–155.
14. Woolrich MW, Ripley BD, Brady M, Smith SM (2001) Temporal autocorrelation in univariate linear modeling of FMRI data. *Neuroimage* 14:1370–1386.
15. Jenkinson M, Smith S (2001) A global optimisation method for robust affine registration of brain images. *Med Image Anal* 5:143–156.
16. Woolrich MW, Behrens TE, Beckmann CF, Jenkinson M, Smith SM (2004) Multilevel linear modelling for FMRI group analysis using Bayesian inference. *Neuroimage* 21: 1732–1747.
17. Nichols TE, Holmes AP (2002) Nonparametric permutation tests for functional neuroimaging: A primer with examples. *Hum Brain Mapp* 15:1–25.
18. Smith SM, Nichols TE (2009) Threshold-free cluster enhancement: Addressing problems of smoothing, threshold dependence and localisation in cluster inference. *Neuroimage* 44:83–98.
19. Naidich TP, et al. (2009) *Duvernoy's Atlas of the Human Brain Stem and Cerebellum* (Springer, New York).
20. O'Doherty JP (2007) Lights, camembert, action! The role of human orbitofrontal cortex in encoding stimuli, rewards, and choices. *Ann N Y Acad Sci* 1121:254–272.

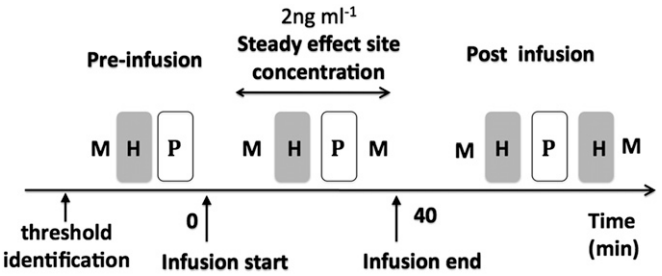

Fig. S1. Experimental paradigm. After identifying the threshold, heat stimulation (H) was performed before, during, and after infusion. Punctate stimulation (P) was performed after every heat stimulation block. Functional scans were performed during noxious stimulation blocks. Mood (M) was assessed before infusing the drug, twice during the infusion, and twice during the postinfusion period. Remifentanil steady-effect site concentration of 2 ng mL^{-1} was maintained for 30 min. Total duration of the infusion was 40 min. Punctate stimuli and all of the measurements after the infusion were for the purpose of investigating opioid-induced hyperalgesia (published elsewhere).

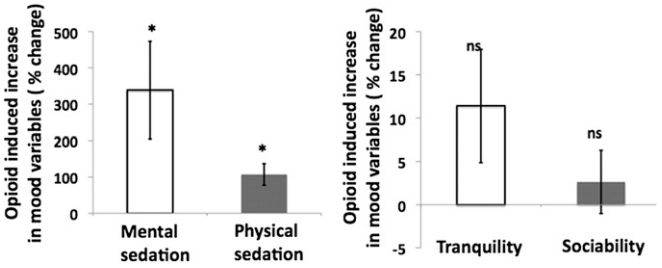

Fig. S2. Opioid-induced increases in mood variables. The *y* axis (*Left* graph) shows the mean opioid-induced increase (as percentage of change) in mental (open bar) and physical (black bar) sedation. The *y* axis (*Right* graph) shows the mean opioid-induced increase (as percentage of change) in tranquility (open bar) and sociability (black bar). Error bars indicate SEM. *$P < 0.01$; NS, not significant ($P > 0.05$). The opioid-induced increase in mood is defined as $[v\ \text{opioid}_{(\text{infusion} - \text{preinfusion})}] - [v\ \text{saline}_{(\text{infusion} - \text{preinfusion})}]$, where v is the mood variable.

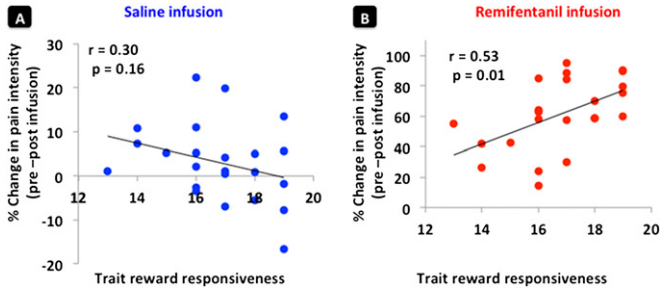

Fig. S3. Relationship between the trait reward responsiveness and changes in pain intensity during the saline (*A*) and remifentanil (*B*) infusions. The *y* axis shows the mean percentage change in pain intensity of noxious heat stimuli from the preinfusion period during each infusion. Trait reward responsiveness (RWR) scores are in the *x* axis. There is a significant positive correlation ($r = 0.53$; $P = 0.01$) between the RWR and the changes in pain intensity induced by the remifentanil infusion. No such relationship is noted during the saline infusion.

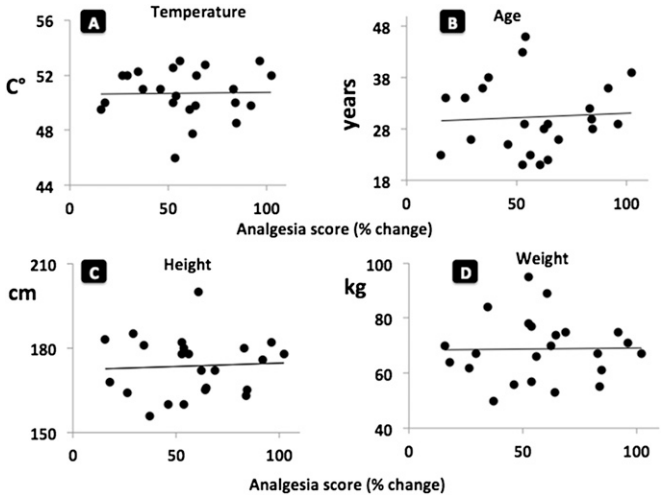

Fig. S4. Absence of influence on opioid-induced analgesia by the temperature used and subject demographics. Analgesia score (percentage of change in pain intensity) in the *x* axis is defined as [*v* opioid$_{(\text{preinfusion} - \text{infusion})}$] − [*v* saline$_{(\text{preinfusion} - \text{infusion})}$], where *v* is pain intensity. (*A*) *Y* axis, temperature used; (*B*) *y* axis, age of the subjects; (*C*) *y* axis, height of the subjects; (*D*) *y* axis, weight of the subjects.

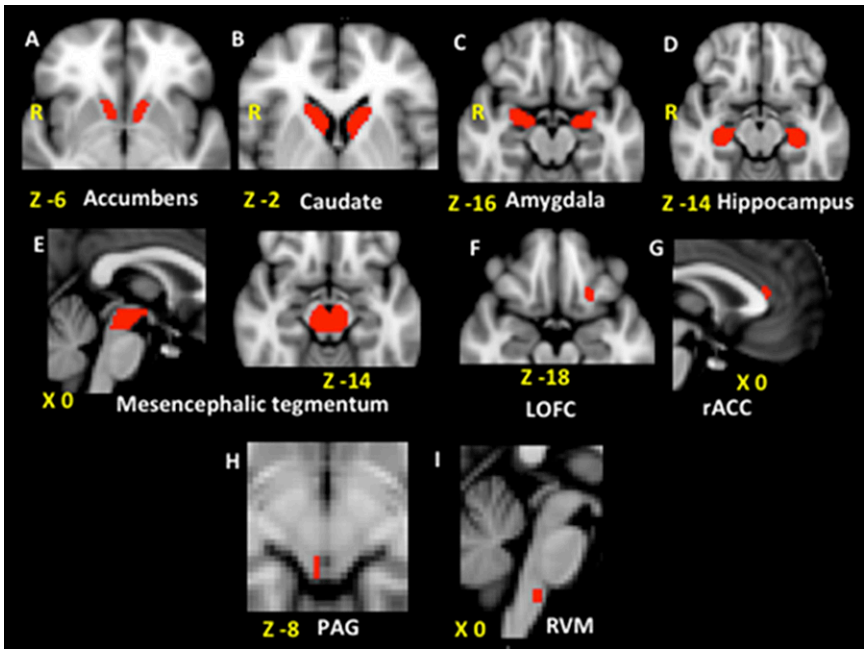

Fig. S5. Masks of the a priori regions of the reward network used for directed searches. Masks are overlaid on a standard structural image. Montreal Neurological Institute (MNI) coordinates are denoted in millimeters below each slice. Masks used for identifying preinfusion period neuronal response to noxious stimuli that predict opioid-induced behavioral analgesia were: right and left nucleus accumbens (*A*), right and left caudate (*B*), right and left amygdala (*C*), right and left hippocampus (*D*), and the mesencephalic tegmentum (*E*). Masks used for identifying areas of the brain where there is a significant positive correlation between the opioid-induced changes in neuronal response to noxious stimuli and opioid-induced behavioral analgesia were: an area of the left orbitofrontal cortex (LOFC) (*F*), an area of rostral anterior cingulate cortex (rACC) (*G*), right and left amygdala (*C*), right and left hippocampus (*D*), right accumbens (*A*), left caudate (*B*), and the mesencephalic tegmentum (*E*). Masks used for identifying areas where there is a significant positive correlation between the preinfusion period neuronal response to noxious stimuli in the ventral tegmental area (VTA) and opioid-induced changes in neuronal response to noxious stimuli were: the left hippocampus (*D*), bilateral amygdala (*C*), an area in the periaqueductal gray (PAG) (*H*), and an area in the rostral ventromedial medulla (RVM) (*I*).

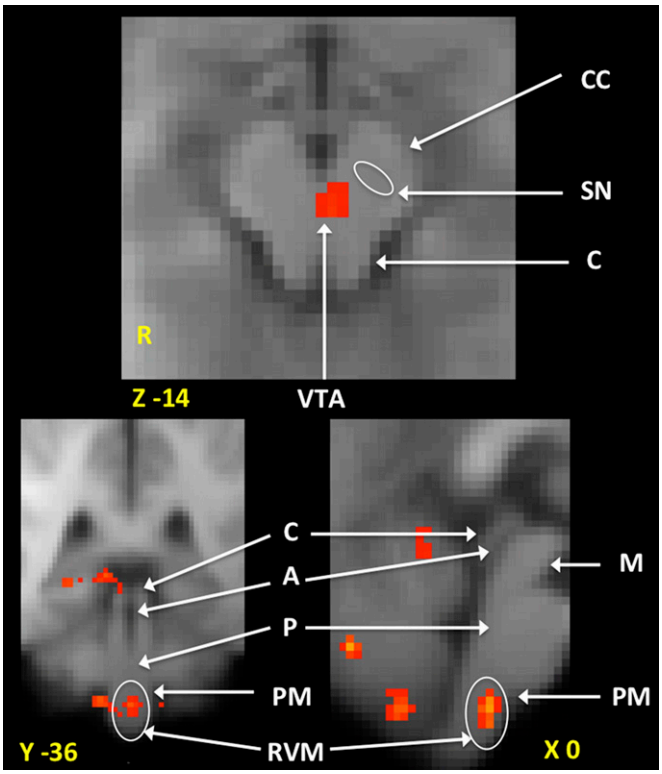

Fig. S6. Localization of the cluster of voxels in the midbrain ventral tegmental area (VTA) and the cluster of voxels in the rostral ventromedial medulla (RVM). The activity is displayed on the group average structural image. Montreal Neurological Institute (MNI) coordinate is indicated in millimeters below the image slices. The cluster of voxels in the VTA (*Upper* image) is where the preinfusion period neuronal response to noxious stimuli predicted opioid-induced behavioral analgesia. See Duvernoy's atlas of the human brainstem and cerebellum (19) to aid identification of anatomical areas. C, colliculi; SN, substantia nigra; CC, crus cerebri. The cluster of voxels in the RVM (*Lower* images) is where opioid-induced changes in neuronal response to noxious stimuli show a significant positive correlation with opioid-induced behavioral analgesia. The activity we observed is in the most rostral and medial aspect of the medulla at the pontomedullary junction as shown by the sagittal image slice on the right and the coronal image slice on the left. The medial and ventral aspects of the rostral medulla in this area contain the nucleus raphe pallidus and the nucleus reticularis gigantocellularis. The image resolution in our results is insufficient to make any claims on activity in specific RVM nuclei. See Duvernoy's atlas of the human brainstem and cerebellum (19) to aid identification of anatomical areas. C, colliculi; A, aqueduct; P, pons in the floor of the IVth ventricle; PM, pontomedullary junction; M, mesencephalon.

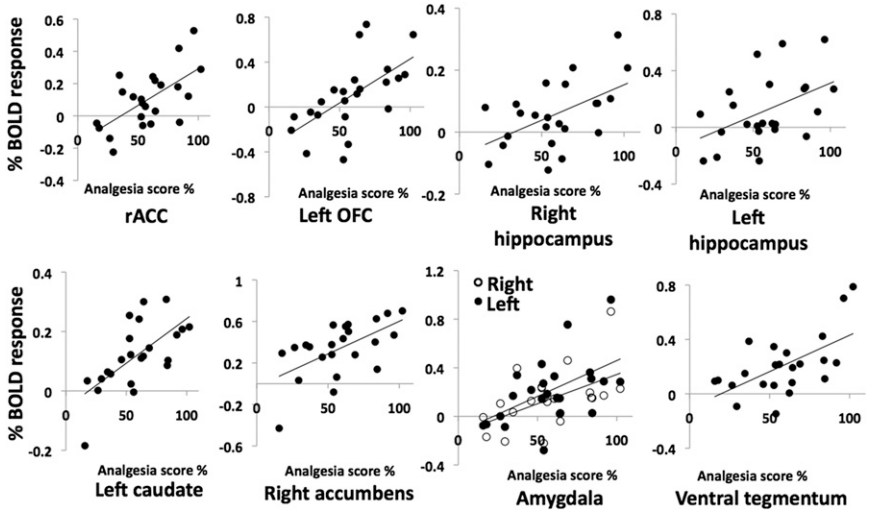

Fig. S7. Scatter plots illustrating the preinfusion period neuronal response to noxious stimuli predicting behavioral analgesia. Preinfusion period neuronal response as percentage of BOLD signal is on the *y* axis. Analgesia score as percentage of change in pain intensity is on the *x* axis. Opioid-induced behavioral analgesia is defined as $[v\ \text{opioid}_{(\text{preinfusion} - \text{infusion})}] - [v\ \text{saline}_{(\text{preinfusion} - \text{infusion})}]$, where *v* is the pain intensity. Percentage of BOLD responses are from the clusters of voxels in areas of the rostral anterior cingulate cortex (rACC), left orbitofrontal cortex, right and left hippocampus (*Upper* row from *Left* to *Right*), the left caudate, right nucleus accumbens, bilateral amygdala (right amygdala in open circles), and the ventral tegmentum (*Lower* row, *Left* to *Right*).

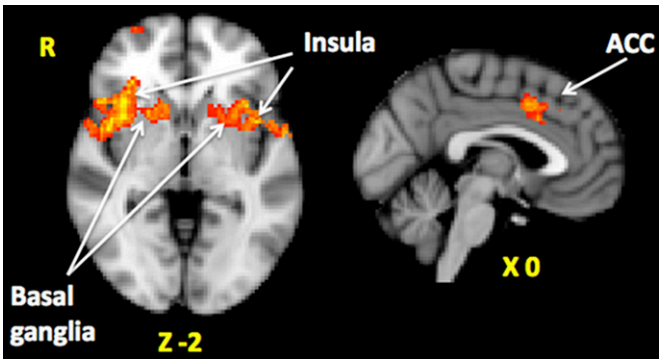

Fig. S8. Areas of the brain with significant opioid-induced reduction in neuronal response to noxious stimuli. Clusters of voxels in areas of the anterior cingulate cortex (ACC), bilateral basal ganglia (putamen and caudate), and insula are shown. Image slices are from the mean statistical map representing significant opioid-induced reductions in neuronal response to noxious stimuli (cluster-based correction: Z score >2.3; $P < 0.05$). Opioid-induced neuronal response is defined as [v opioid$_{(\text{preinfusion} - \text{infusion})}$] − [$v$ saline$_{(\text{preinfusion} - \text{infusion})}$], where v is the neuronal response to noxious stimuli. Montreal Neurological Institute coordinates are denoted in millimeters below each slice.

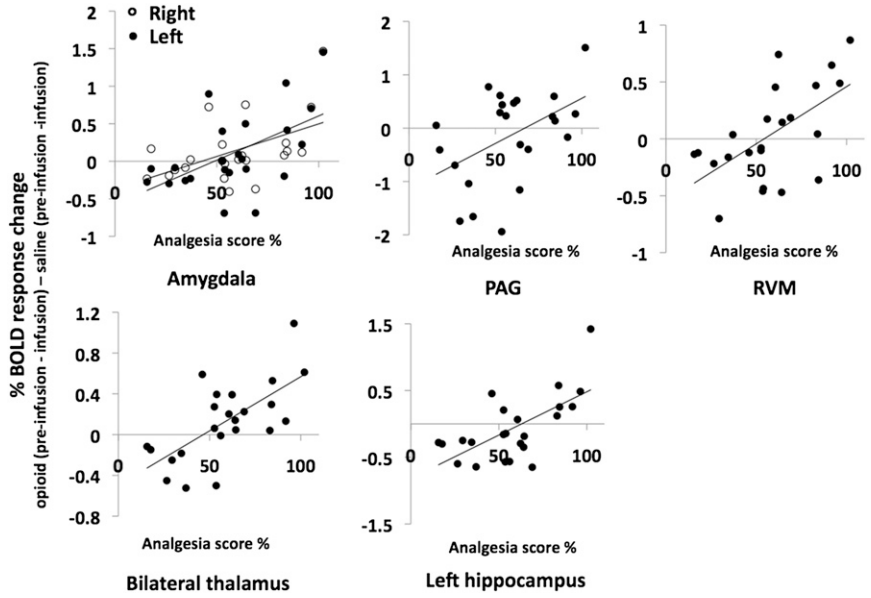

Fig. S9. Scatter plots illustrating the significant positive correlation between opioid-induced behavioral analgesia and opioid-induced changes in neuronal response to noxious stimuli. Opioid-induced changes in neuronal response (percentage of BOLD response) and analgesia (percentage of change in pain intensity) are defined as [v opioid$_{(\text{preinfusion} - \text{infusion})}$] − [$v$ saline$_{(\text{preinfusion} - \text{infusion})}$], where v is the percentage of BOLD response or the pain intensity of noxious stimuli. A positive value for the change in percentage of BOLD response indicates an opioid-induced reduction in the neuronal response. Opioid-induced change in neuronal response as percentage of BOLD response change is on the y axis. Analgesia score as percentage of change in pain intensity is on the x axis. Percentage of BOLD response changes are from the clusters of voxels in areas of the bilateral amygdala (right amygdala in open circles), periaqueductal gray (PAG), rostral ventromedial medulla (RVM) (*Upper* row from *Left* to *Right*), bilateral thalamus, and left hippocampus (*Lower* row, *Left* to *Right*).